

# Imposition of physical parameters in dissipative particle dynamics

N. Mai-Duy<sup>1,\*</sup>, N. Phan-Thien<sup>2</sup> and T. Tran-Cong<sup>1</sup>

<sup>1</sup>Computational Engineering and Science Research Centre,

School of Mechanical and Electrical Engineering,

University of Southern Queensland, Toowoomba, QLD 4350, Australia

<sup>2</sup> Department of Mechanical Engineering, Faculty of Engineering,

National University of Singapore, 9 Engineering Drive 1, 117575, Singapore.

Submitted to *Computer Physics Communications*, February/2017; Revised (1), May/2017; Revised (2), June/2017; Revised (3), August/2017

ABSTRACT: In the mesoscale simulations by the dissipative particle dynamics (DPD), the motion of a fluid is modelled by a set of particles interacting in a pairwise manner, and it has been shown to be governed by the Navier-Stokes equation, with its physical properties, such as viscosity, Schmidt number, isothermal compressibility, relaxation and inertia time scales, etc., in fact its whole rheology resulted from the choice of the DPD model parameters. In this work, we will explore the response of a DPD fluid with respect to its parameter space, where the model input parameters can be chosen in advance so that (i) the ratio between the relaxation and inertia time scales is fixed; (ii) the isothermal compressibility of water at room temperature is enforced; and (iii) the viscosity and Schmidt number can be specified as inputs. These impositions are possible with some extra degrees of freedom in the weighting functions for the conservative and dissipative forces. Numerical experiments show an improvement in the solution quality over conventional DPD parameters/weighting functions, particularly for the number density distribution and computed stresses.

Keywords: Dissipative particle dynamics, physical/dimensionless parameters, weighting functions, inertia and relaxation time scales, compressibility, viscosity, dynamic response.

---

\*Corresponding author E-mail: [nam.mai-duy@usq.edu.au](mailto:nam.mai-duy@usq.edu.au), Telephone +61-7-46312748, Fax +61-7-46312529

# 1 Introduction

Dissipative particle dynamics (DPD) has become a popular numerical tool for probing the behaviour of complex fluids at a mesoscopic length scale (e.g. polymeric/colloidal fluids), (see, e.g., [1,2,3,4,5,6,7]). In DPD, the fluid is replaced by a set of particles (called DPD particles) undergoing their Newton 2nd law of motion while interacting in a pairwise manner. There are three typical types of interaction forces between DPD particles, a conservative force used to model local thermodynamics, a dissipative force used to model viscous actions, and a random force to provide a balance to the dissipative force, to maintain a constant specific kinetic energy (defined as the Boltzmann temperature). All forces are pairwise and centre-to-centre. DPD has a sound statistical foundation: it is shown to satisfy conservations of mass and momentum in the mean [8,9]. The input parameters of DPD include a noise level  $\sigma$ , Boltzmann temperature  $k_B T$ , repulsion strength  $a_{ij}$ , number density  $n$ , particle's mass  $m$  and cut-off radius  $r_c$  (which may be different for conservative and dissipative forces). It is noted that a friction coefficient  $\gamma$  is derived from the noise level through the fluctuation-dissipation theorem; it is not an independent input. For the scaling in DPD, a physical system represented by  $N_{phys}$  “molecular particles” can be scaled (coarse-grained) at different levels  $\nu$  so that one deals with a smaller number of particles  $N = N_{phys}/\nu$  in which  $\nu$  is referred to as the coarse-grained level [10]. Let  $\nu$  (modelled by  $\{N, k_B T, n, m, r_c, a_{ij}, \gamma\}$ ) and  $\nu'$  ( $\{N', k_B T', n', m', r'_c, a'_{ij}, \gamma'\}$ ) be two different coarse-grained levels; both represent the same physical fluid. By constraining the compressibility of the coarse-grained level fluids, it was shown that if two different coarse-grained levels are related by ( $\phi$  is the scaling)

$$N' = \phi^{-1}N, \quad k_B T' = \phi k_B T, \quad n' = \phi^{-1}n, \quad (1)$$

then

$$\begin{aligned} m' &= \phi m, & r'_c &= \phi^{1/3} r_c, & \tau' &= \phi^{1/3} \tau, \\ a'_{ij} &= \phi^{2/3} a_{ij}, & \gamma' &= \phi^{2/3} \gamma, & \sigma' &= \phi^{5/6} \sigma, \end{aligned} \quad (2)$$

in which  $\tau = r_c \sqrt{m/k_B T}$  and  $\tau' = r'_c \sqrt{m'/k_B T'}$  are time scalings. Under these scalings, one can show that the two coarse-grained systems are equivalent (i.e. the scale free property).

There are several issues in the classical DPD method. The physical parameters of the fluid

to be modelled are not inputs of the DPD system, making its parametric study difficult. Any change in the input model parameters (e.g. the cut-off radius and Boltzmann temperature) may result in a different fluid. Although the scheme defined by (1) and (2) allows of the use of  $\nu$  larger than 1, it does not provide an appropriate link between the scaling and thermal fluctuations to ensure that the fluctuations will reduce their magnitude when the coarse-grained level increases. Also, the method always produces a local pressure as a quadratic function of the number density (i.e. a fixed equation of state), and does not inherit the feature of “mesh/grid convergence” from conventional discretisation methods. There is still no formal way of deriving DPD from an atomistic system for simple fluids (unbonded atoms). On the other hand, DPD possesses an algorithmic simplicity and has the ability to model many different complex fluids. Indeed, objects suspended in the fluid can also be represented by DPD particles with appropriate forms of interactions. For example, a solid particle can be modelled by a single DPD particle [5] or by a few constrained basic DPD particles [7], allowing of efficient simulations of particulate suspensions [5,7,11], and of thixotropic materials exhibiting pseudo yield stress behaviour [12] to be carried out. When the atoms are bonded (e.g. complex molecules like proteins), the coarse-grained mapping can be well defined and there have been many attempts in DPD modelling to explore flows of such fluids [13,14]; here the DPD method can be regarded as a bottom-up approach. In contrast to DPD, the smoothed DPD (sDPD) method [18] is directly derived from the Navier-Stokes equation with the inclusion of thermal fluctuations (i.e. a top-down approach). Its formulation thus combines the advantages of the Navier-Stokes equation (i.e. an arbitrary equation of state, specified viscosity and convergence property) and the DPD (i.e. mesoscopic description). Each sDPD particle is defined with an explicit volume. For the scaling in sDPD, it was shown in [15] that the deterministic part is scale invariant and the thermal fluctuation part has a consistent scaling with the volume of fluid particles. The reader is referred to [16] for a recent comprehensive review of the field.

In DPDs, the compressibility of the model fluid is set to match the compressibility of water

at room temperature, resulting in a constraint to the repulsion strength [17]

$$a_{ij} = \frac{71.54k_B T}{nr_c^4} \quad \text{for 3D case,} \quad (3)$$

$$a_{ij} = \frac{57.23k_B T}{nr_c^3} \quad \text{for 2D case,} \quad (4)$$

revealing the dependence of  $a_{ij}$  on  $k_B T$ ,  $n$  and  $r_c$ . In [18], it was shown that the friction coefficient can be chosen to fix the viscosity of the system. In [17,19,20,21,22], the dynamic response of a DPD fluid, measured by the Schmidt number (the ratio between momentum diffusion (viscosity) and mass diffusivity) was discussed. In this study, apart from the physical parameters just mentioned, another dimensionless parameter, i.e. the ratio between the inertia and relaxation time scales of the DPD equations, will also be considered. This parameter provides a direct link between the conservative and dissipative forces; it governs how fast the system approaches the statistical equilibrium state, together with the clustering of particles, and therefore an appropriate value of this ratio helps stabilise the density distribution of DPD particles in the flow domain.

We will examine the response of a DPD fluid to a flow condition in the following two forms. In the first, there are two dimensionless quantities (time-scale ratio and isothermal compressibility) to be imposed. The method here is basically the same as conventional DPDs, except that its conservative force involves two free parameters (instead of one). In the second, three dimensionless quantities (time-scale ratio, isothermal compressibility and Schmidt number), and the viscosity are to be enforced. These simultaneous impositions are possible by modifying both the weighting functions of the conservative and dissipative forces. Some simulations are carried out in viscometric flows to illustrate the advantages of the proposed DPD fluid.

The structure of the paper is organised as follows. In section 2, brief overviews of the DPD equations and their associated standard input values are given. In section 3, numerical issues concerning the time scales in the DPD equations are discussed. In section 4, the response of the DPD system under constraints of satisfying some given physical/dimensionless parameters of the fluid concerned is examined. Section 5 gives some concluding remarks.

## 2 DPD model

### 2.1 Equations

In DPD, the fluid is modelled by a system of particles undergoing their Newton 2nd law motion:

$$m_i \ddot{\mathbf{r}}_i = m_i \dot{\mathbf{v}}_i = \sum_{j=1, j \neq i}^N (\mathbf{F}_{ij,C} + \mathbf{F}_{ij,D} + \mathbf{F}_{ij,R}), \quad (5)$$

where  $m_i$ ,  $\mathbf{r}_i$  and  $\mathbf{v}_i$  represent the mass, position vector and velocity vector of a particle  $i = 1, \dots, N$ , respectively,  $N$  is the total number of particles, the superposed dot denotes a time derivative, and the three forces on the right side of (5) represent the conservative force (subscript C), the dissipative force (subscript D) and the random force (subscript R):

$$\mathbf{F}_{ij,C} = a_{ij} w_C \mathbf{e}_{ij}, \quad (6)$$

$$\mathbf{F}_{ij,D} = -\gamma w_D (\mathbf{e}_{ij} \cdot \mathbf{v}_{ij}) \mathbf{e}_{ij}, \quad (7)$$

$$\mathbf{F}_{ij,R} = \sigma w_R \theta_{ij} \mathbf{e}_{ij}, \quad w_R = \sqrt{w_D}, \quad \sigma = \sqrt{2\gamma k_B T}, \quad (8)$$

where  $a_{ij}$ ,  $\gamma$  and  $\sigma$  are constants reflecting the strengths of these forces,  $w_C$ ,  $w_D$  and  $w_R$  configuration-dependent weighting functions,  $\mathbf{e}_{ij} = \mathbf{r}_{ij}/r_{ij}$  a unit vector from particle  $j$  to particle  $i$  ( $\mathbf{r}_{ij} = \mathbf{r}_i - \mathbf{r}_j$ ,  $r_{ij} = |\mathbf{r}_{ij}|$ ),  $\mathbf{v}_{ij} = \mathbf{v}_i - \mathbf{v}_j$  a relative velocity vector, and  $\theta_{ij}$  a Gaussian white noise. It is noted that the random force is introduced in a way that satisfies the fluctuation-dissipation theorem.

### 2.2 Standard input values

Groot and Warren [17] suggested that the noise level  $\sigma$  can be chosen as a balance between a fast simulation and a good satisfaction of the specified Boltzmann temperature - a value of 3 was recommended (for  $k_B T = 1$ , the corresponding  $\gamma$  is 4.5). They also recommended that the repulsion strength  $a_{ij}$  is chosen such that a DPD fluid has the same compressibility as water at room temperature. This results in the constraints (3) and (4). As discussed in

Section 1, a relatively small number of particles can be chosen to represent the fluid. In practice, the number density  $n = 4$  has been widely used.

For conventional DPDs, the weighting functions are given by

$$w_C = 1 - \frac{r_{ij}}{r_c}, \quad (9)$$

$$w_D = \left(1 - \frac{r_{ij}}{r_c}\right)^2. \quad (10)$$

It is noted that the exponent in  $w_D$  is also often taken as 1/2 (rather than 2), with a resulting improve in response of the fluid. In this study, the value of 1/2 is employed for the conventional DPD.

### 3 Time scales

Let us focus on a tagged, but otherwise arbitrary DPD particle in the system, and let  $\tau$  be its relaxation time scale,  $\tau_I$  its inertia time scale and  $\alpha$  the ratio of the two time scales

$$\tau = O\left(\frac{\gamma}{H}\right) = O\left(\frac{\gamma r_c}{a_{ij}}\right), \quad (11)$$

$$\tau_I = O\left(\frac{m}{\gamma}\right), \quad (12)$$

$$\alpha = \frac{\tau}{\tau_I} = O\left(\frac{\gamma^2 r_c}{m a_{ij}}\right), \quad (13)$$

where  $H$  is the stiffness defined as

$$H = O(|\partial_r F_C|) = O\left(\frac{a_{ij}}{r_c}\right). \quad (14)$$

Substitution of (3) and (4) into (13) yield, respectively,

$$\alpha = \frac{\tau}{\tau_I} \sim \frac{\gamma^2 r_c^5 n}{71.54 m k_B T}, \quad \text{for 3D space,} \quad (15)$$

$$\alpha = \frac{\tau}{\tau_I} \sim \frac{\gamma^2 r_c^4 n}{57.23 m k_B T}, \quad \text{for 2D space.} \quad (16)$$

It can be seen that the dimensionless quantity  $\alpha$  is a function of  $m, r_c, n, \gamma$  and  $k_B T$ .

For the case of a small  $m$  (small  $\tau_I$ , large  $\alpha$ ), the particles' inertia can be neglected leading to a fast response. Small time steps are required for a numerical simulation, but particles are well distributed because of a low Mach number. A stochastic exponential-time differencing (SETD) scheme is shown to be an efficient solver. As  $m \rightarrow 0$ , the DPD equations become singular due to the loss of their highest time derivative terms, and special numerical treatments are required. Detailed discussions can be found in [23,24,25].

In our current investigation, we keep the mass and number density fixed ( $m = 1$  and  $n = 4$ ) and vary the cut-off radius ( $r_c \geq 1$ ).

With standard DPD input values ( $m = 1, k_B T = 1, n = 4, \sigma = 3$  ( $\gamma = 4.5$ ),  $r_c = 1$ ), where the DPD system is observed to well behave, the ratio between the two time scales can be estimated as

$$\alpha = \frac{\tau}{\tau_I} \sim 1.1322 = O(1), \quad \text{for 3D space,} \quad (17)$$

$$\alpha = \frac{\tau}{\tau_I} \sim 1.4153 = O(1), \quad \text{for 2D space.} \quad (18)$$

Expressions (15) and (16) indicate that  $r_c$  has a very strong influence on the time-scale ratio. For example, with  $r_c = 2.5$ , one has  $\alpha = O(10^2)$ . Also, as  $r_c$  increases from 1 to 2.5,  $a_{ij}$ , from (4), is reduced from 14.30 to 0.91. Figure 1 displays the spatial configurations of DPD particles at an instant, for  $r_c = 1$  and  $r_c = 2.5$ , from which it can be seen that particles tend to form local clusters as  $r_c$  increases ( $a_{ij}$  decreases). It appears that a large value of  $\alpha$ , due to large  $r_c$ , may adversely affect the stability of the DPD system through clustering. Our recommendation here is to make  $\alpha$  constant (independently of the input parameters) and having an appropriate value to avoid the clustering of particles. The optimal value of  $\alpha$  is to be determined numerically.

## 4 Imposition of physical/dimensionless parameters

### 4.1 Dimensionless compressibility and time-scale ratio

Our goal here is to create a new form of the conservative force that can control both the isothermal compressibility and time scale ratio. To do so, apart from  $a_{ij}$ , there is a need for having another free parameter. A conservative force is proposed to be

$$F_{ij,C} = a_{ij} \left(1 - \frac{r}{r_c}\right)^{\bar{s}}, \quad \bar{s} > 0, \quad (19)$$

whose average gradient over  $0 \leq r \leq r_c$  is also  $a_{ij}/r_c$ . These two free parameters,  $a_{ij}$  and  $\bar{s}$ , can be designed to satisfy

$$\alpha = \frac{\tau}{\tau_I} = \frac{\gamma^2 r_c}{m a_{ij}}, \quad (20)$$

$$\kappa^{-1} = \frac{1}{k_B T} \frac{\partial p}{\partial n}, \quad (21)$$

where  $p$  and  $\kappa$  are the pressure and isothermal compressibility, respectively ( $\alpha$  and  $\kappa$  are given constants, e.g., for water,  $\kappa = 1/15.98$ ).

From the virial theorem, the pressure is computed as

$$p = nk_B T + \frac{n^2}{2d} \int d\mathbf{R} r F_{ij,C}(r) g(r), \quad (22)$$

where  $g(r)$  is the radial distribution function and  $d$  the flow dimensionality. Here, we simply take  $g(r) = 1$  corresponding to an infinite number of DPD particles.

Expression (22) results in

$$p = nk_B T + \frac{1}{2} \frac{n^2}{3} \int_0^{r_c} 4\pi r^2 dr \left[ r a_{ij} \left(1 - \frac{r}{r_c}\right)^{\bar{s}} \right], \quad (23)$$

$$= nk_B T + \frac{4\pi a_{ij} n^2 r_c^4}{(\bar{s} + 1)(\bar{s} + 2)(\bar{s} + 3)(\bar{s} + 4)}, \quad (24)$$

$$\frac{\partial p}{\partial n} = k_B T + \frac{8\pi a_{ij} n r_c^4}{(\bar{s} + 1)(\bar{s} + 2)(\bar{s} + 3)(\bar{s} + 4)}, \quad (25)$$



for 3D case, and

$$p = nk_B T + \frac{1}{2} \frac{n^2}{2} \int_0^{r_c} 2\pi r dr \left[ r a_{ij} \left( 1 - \frac{r}{r_c} \right)^{\bar{s}} \right], \quad (26)$$

$$= nk_B T + \frac{\pi a_{ij} n^2 r_c^3}{(\bar{s} + 1)(\bar{s} + 2)(\bar{s} + 3)}, \quad (27)$$

$$\frac{\partial p}{\partial n} = k_B T + \frac{2\pi a_{ij} n r_c^3}{(\bar{s} + 1)(\bar{s} + 2)(\bar{s} + 3)}, \quad (28)$$

for 2D case. Equations (25) and (28) for the variable  $\bar{s}$  can be solved analytically and we are interested in only physical positive values of  $\bar{s}$ .

Analytic solution to (20) and (21) can thus be found as

$$a_{ij} = \frac{1}{\alpha} \frac{\gamma^2 r_c}{m}, \quad (29)$$

$$\bar{s} = \frac{\sqrt{5 + 4\sqrt{C + 1}} - 5}{2}, \quad C = \frac{8\pi a_{ij} n r_c^4}{(\kappa^{-1} - 1)k_B T}, \quad (30)$$

for 3D space, and

$$a_{ij} = \frac{1}{\alpha} \frac{\gamma^2 r_c}{m}, \quad (31)$$

$$\bar{s} = \frac{1}{3B} + B - 2, \quad B = \left( \frac{C}{2} + \sqrt{\frac{C^2}{4} - \frac{1}{27}} \right)^{1/3}, \quad C = \frac{2\pi a_{ij} n r_c^3}{(\kappa^{-1} - 1)k_B T}, \quad (32)$$

for 2D space. For (30) and (32) to have a physical value (i.e.  $\bar{s} > 0$ ), it requires that  $C > 24$  and  $C > 6$ , respectively, which can be easily satisfied.

Alternatively, the condition of isothermal compressibility can be replaced with the speed of sound

$$c_s^2 = \frac{\partial p}{\partial \rho}, \quad (33)$$

where  $\rho = mn$  is the density. The corresponding  $a_{ij}$  and  $\bar{s}$  have the same forms as (29)-(30) and (31)-(32), except that values of  $C$  in (30) and (32) are replaced with  $8\pi a_{ij} n r_c^4 / (m c_s^2 - k_B T)$  and  $2\pi a_{ij} n r_c^3 / (m c_s^2 - k_B T)$ , respectively.

## 4.2 Viscosity and dynamic response

The fluid viscosity and its dynamic response (via the Schmidt number) can be prescribed as input parameters of the DPD equations. Discussions were given in [18,22] from a smoothed DPD perspective. Here, we present the formulation from a DPD perspective.

Following [26], we employ (note no overbar on  $s$ )

$$w_D = \left(1 - \frac{r}{r_c}\right)^s, \quad s > 0. \quad (34)$$

The dissipative force now involves 2 free parameters,  $\gamma$  and  $s$ , and we utilise them to match two thermodynamic properties (i.e. flow resistance and dynamic response). Note that  $s$  and  $\bar{s}$  are two different parameters, one used for the dissipative force and one for the conservative force.

By means of kinetic theory, expressions for the dynamic viscosity and Schmidt number have been derived as, in a similar manner to [4],

$$\bar{\eta} = \bar{\eta}_K + \bar{\eta}_D = \frac{dmk_B T}{2\gamma[w_D]_R} + \frac{\gamma n^2 [R^2 w_D]_R}{2d(d+2)}, \quad (35)$$

$$\bar{S}_c = \frac{\bar{\eta}}{\rho D}, \quad D = \frac{2\bar{\eta}_K}{\rho}, \quad (36)$$

where  $d$  is the number of dimensions,  $D$  the diffusion coefficient,  $[w_D]_R = \int d\mathbf{R} w_D(R)$  and  $[R^2 w_D]_R = \int d\mathbf{R} R^2 w_D(R)$ . With  $w_D$  containing a free parameter  $s$  (34), it can be shown that

$$[w_D]_R = \frac{8\pi r_c^3}{(s+1)(s+2)(s+3)}, \quad [R^2 w_D]_R = \frac{96\pi r_c^5}{(s+1)(s+2)(s+3)(s+4)(s+5)}, \quad 3D, \quad (37)$$

$$[w_D]_R = \frac{2\pi r_c^2}{(s+1)(s+2)}, \quad [R^2 w_D]_R = \frac{12\pi r_c^4}{(s+1)(s+2)(s+3)(s+4)}, \quad 2D. \quad (38)$$

In (35), there are two contributions to the viscosity, the kinetic part  $\bar{\eta}_K$  (gaseous contribution) and the dissipative part  $\bar{\eta}_D$  (liquid contribution). Here, we are interested in the case where the dissipative contribution is a dominant part, i.e.  $\bar{\eta}_D \gg \bar{\eta}_K$  (liquid-like behaviour)

under which the two following constraints are approximately satisfied

$$\bar{\eta}_D = \eta, \quad (39)$$

$$\frac{\bar{\eta}_D}{\bar{\eta}_K} = 2S_c, \quad (40)$$

or

$$\frac{\gamma n^2 [R^2 w_D]_R}{2d(d+2)} = \eta, \quad (41)$$

$$\frac{2\gamma\eta [w_D]_R}{dmk_B T} = 2S_c. \quad (42)$$

This system can be solved analytically for the two variables  $\gamma$  and  $s$ . In 3D space, the solution to the system is

$$s = \frac{-9 + \sqrt{1 + 4C}}{2}, \quad C = \frac{6S_c m k_B T n^2 r_c^2}{5\eta^2}, \quad (43)$$

$$\gamma = \frac{5\eta(s+1)(s+2)(s+3)(s+4)(s+5)}{16\pi n^2 r_c^5}. \quad (44)$$

Since  $s > 0$ , it requires

$$\eta < \sqrt{\frac{3S_c m k_B T n^2 r_c^2}{50}} \quad \text{for a given } S_c, \quad (45)$$

$$S_c > \frac{50\eta^2}{3m k_B T n^2 r_c^2} \quad \text{for a given } \eta. \quad (46)$$

In 2D, the solution to the system takes the form

$$s = \frac{-7 + \sqrt{1 + 4C}}{2}, \quad C = \frac{3S_c m k_B T n^2 r_c^2}{4\eta^2}, \quad (47)$$

$$\gamma = \frac{4\eta(s+1)(s+2)(s+3)(s+4)}{3\pi n^2 r_c^4}. \quad (48)$$

Since  $s > 0$ , it requires

$$\eta < \sqrt{\frac{S_c m k_B T n^2 r_c^2}{16}} \quad \text{for a given } S_c, \quad (49)$$

$$S_c > \frac{16\eta^2}{m k_B T n^2 r_c^2} \quad \text{for a given } \eta. \quad (50)$$

### 4.3 Isothermal compressibility and time-scale ratio as specified inputs

The method implemented here is the conventional DPD with its conservative force in the form of (19) instead of (9). The friction coefficient/noise level is a specified input. Simulation is conducted on Couette flow. We estimate the optimal value of  $\alpha$  numerically. Results obtained are examined through the variation of the number density  $n$  and shear stress  $\tau_{xy}$  on the cross section of the flow.

Results concerning the standard deviation of  $n$  and  $\tau_{xy}$  on the cross section for  $\alpha = (500, 50, 5, 0.5, 0.05, 0.005, 0.0005)$  are shown in Figure 2, showing that the best  $\alpha$  corresponding the smallest variation of  $\tau_{xy}$  and  $n$  is in the range of  $10^{-1}$  to  $10^{+1}$ . The distribution of particles over the flow domain is displayed for  $\alpha = 0.0005$  and  $\alpha = 0.5$  in Figure 3, showing that particles tend to form local clusters at  $\alpha = 0.0005$ . For simplicity,  $\alpha = 1$  is considered here as a good choice.

Table 1 compares DPD results between the proposed conservative force ( $\alpha = 1$ ) and conventional one for several values of  $r_c$ . For all cases, variations of the number density and shear stress on the flow cross section are considerably smaller with the proposed conservative force. It is noted that different fluids are considered here, e.g., viscosity at  $r_c = 4$  is much greater than viscosity at  $r_c = 2$ . Figure 4 displays some typical DPD results, including temperature, velocities and stresses. It can be seen that the two DPD systems have a Newtonian response (zero normal stress difference and constant shear stress). However, with the proposed conservative force, much more stable results for the spatial configuration, number density and shear stress on the cross section are observed.

### 4.4 Isothermal compressibility, times-scale ratio, dynamic response and viscosity as specified inputs

These four parameters are prescribed to be inputs of DPD equations. They define a particular fluid; but unlike conventional DPDs, a change in  $r_c$  should not affect the fluid characteristics.

For a given shear rate  $\dot{\gamma}$ , shear stresses in Couette flow can be computed as  $\tau_{xy} = \eta\dot{\gamma}$  and these “exact values” are used to assess the accuracy of the present DPD.

First, for a typical set of input parameters, we plot the standard deviations of  $n$  and  $\tau_{xy}$  on the cross section and percentage errors of  $\tau_{xy}$  against the time-scale ratio  $\alpha$  (Figure 5). It can be seen that the minimum values of variations and percentage errors occur within  $\alpha$  range of  $10^{-1}$  to  $10^1$ . This range is the same as in the case of friction coefficient as a specified input. We will choose  $\alpha = 1$  for simplicity.

To examine the effects of enforcing the fixed time scale ratio  $\alpha = 1$ , the obtained results are compared with those by the DPD, where the conventional conservative force is implemented (i.e. variable  $\alpha$ ). Table 2 indicates that a solution by the proposed conservative force (fixed  $\alpha$ ) is more stable and accurate than a solution by the conventional conservative force (variable  $\alpha$ ) for several values of  $r_c$ . Table 3 reveals that the viscosity estimated by the Kirkwood-Irving formulation is closer to a specified input value with the proposed conservative force. Figure 6 shows that the proposed conservative force also results in a more stable spatial configuration, number density and shear stress on the cross section. In comparison with Figure 4, for the same  $r_c$ , DPD results with  $\eta$  and  $S_c$  as specified inputs are superior (smaller variations) to those with  $\gamma$  as a specified input.

## 5 Concluding remarks

The DPD method has received a great deal of attention in the last two decades with various reported modelling applications involving complex fluids. Its algorithmic simplicity comes at the expense of several shortcomings, including a fixed (quadratic) form of the equation of state, no formal way of deriving DPD from an atomistic system for simple fluids (unbonded atoms), and an indirect connection between the physical and model parameters which causes difficulty in studying the effects of some input parameters such as  $r_c$ ,  $k_B T$  and  $n$ . This paper is concerned with the question of how to impose some physical/dimensionless parameters of the fluid on the DPD model. [The proposed scheme for imposing the viscosity and Schmidt](#)

number is derived from the kinetic theory, where the conservative force is set to zero and the corresponding equation of state is that of an ideal gas. Expressions for the physical parameters are provided in analytic form and they are supported by numerical results, including conservative forces. The method offers a more meaningful way to conduct a DPD simulation which yields a more stable solution over the change in the model inputs. The proposed DPD formulation can be combined in a straightforward manner with exiting models of suspended phases in DPD to simulate complex fluids.

## References

1. P.J. Hoogerbrugge, J.M.V.A. Koelman, *Europhys. Lett.* 19(3) (1992) 155-160
2. Y. Kong, C.W. Manke, W.G. Madden, A.G. Schlijper, *J. Chem. Phys.* 107 (1997) 592-602
3. M. Laradji, M.J.A. Hore, *J. Chem. Phys.* 121 (2004) 10641-10647
4. C.A. Marsh, *Theoretical Aspects of Dissipative Particle Dynamics* (D. Phil. Thesis), University of Oxford, 1998
5. W. Pan, B. Caswell, G.E. Karniadakis, *Langmuir* 26(1) (2010) 133-142
6. N. Phan-Thien, *Understanding Viscoelasticity: An Introduction to Rheology*, second ed., Springer, Berlin, 2013
7. N. Phan-Thien, N. Mai-Duy, B.C. Khoo, *J. Rheol.* 58 (2014) 839-867
8. P. Español, *Phys. Rev. E* 52 (1995) 1734-1742
9. P. Español, P. Warren, *Europhys. Lett.* 30(4) (1995) 191-196
10. R.M. Fuchsli, H. Fellermann, A. Eriksson, H.-J. Ziock, *J. Chem. Phys.* 130 (2009) 214102
11. N. Mai-Duy, N. Phan-Thien, B.C. Khoo, *Comput. Phys. Comm.* 189 (2015) 37-46
12. K. Le-Cao, N. Phan-Thien, B.C. Khoo, N. Mai-Duy, *Journal of Non-Newtonian Fluid Mechanics* 241 (2017) 1-13

13. P. Español, Phys. Rev. E 53(2) (1996) 1572-1578
14. Z. Li, X. Bian, B. Caswell, G.E. Karniadakis, Soft Matter 10(43) (2014) 8659-8672
15. A. Vázquez-Quesada, M. Ellero, P. Español, J. Chem. Phys. 130(3) (2009) 034901
16. P. Español, P.B. Warren, J. Chem. Phys. 146(15) (2017) 150901
17. R.D. Groot, P.B. Warren, J. Chem. Phys. 107 (1997) 4423
18. P. Español, M. Revenga, Phys. Rev. E 67(2) (2003) 026705
19. S. Litvinov, M. Ellero, X. Hu, N.A. Adams, J. Chem. Phys. 130 (2009) 021101
20. S. Litvinov, M. Ellero, X. Hu, N.A. Adams, J. Comput. Phys. 229(15) (2010) 5457-5464
21. V. Symeonidis, G.E. Karniadakis, B. Caswell, J. Chem. Phys. 125 (2006) 184902
22. N. Mai-Duy, N. Phan-Thien, T. Tran-Cong, Applied Mathematical Modelling 46 (2017) 602-617
23. N. Mai-Duy, N. Phan-Thien, B.C. Khoo, J. Comput. Phys. 245 (2013) 150-159
24. N. Phan-Thien, N. Mai-Duy, D. Pan, B.C. Khoo, Comput. Phys. Comm. 185(1) (2014) 229-235
25. N. Phan-Thien, N. Mai-Duy, B.C. Khoo, D. Duong-Hong, Applied Mathematical Modelling 40(13-14) (2016) 6359-6375
26. X. Fan, N. Phan-Thien, S. Chen, X. Wu, T.Y. Ng, Phys. Fluids 18(6) (2006) 063102

Table 1: Couette flow, friction coefficient as specified input,  $\gamma = 4.5$ ,  $m = 1$ ,  $k_B T = 1$ ,  $n = 4$ ,  $\Delta t = 0.001$ , compressibility of water, shear rate of 0.2: Mean and standard deviation of the number density  $n$  and shear stress  $\tau_{xy}$  on the cross section of the flow for several values of  $r_c$  by the proposed ( $\alpha = 1$ ) and conventional conservative forces using the same number of time steps. For a given  $r_c$ , the variation in the DPD results is significantly reduced with the modified conservative force. Note that different values of  $r_c$  correspond to different fluids.

	$r_c = 2$			
	mean( $n$ )	std( $n$ )	mean( $\tau_{xy}$ )	std( $\tau_{xy}$ )
Conventional $F_C$	4	0.3896	8.8371	1.1373
Proposed $F_C$	4	0.2269	9.1572	0.7805
	$r_c = 2.5$			
	mean( $n$ )	std( $n$ )	mean( $\tau_{xy}$ )	std( $\tau_{xy}$ )
Conventional $F_C$	4	0.6104	22.1690	3.0665
Proposed $F_C$	4	0.2991	22.5067	1.8567
	$r_c = 3.0$			
	mean( $n$ )	std( $n$ )	mean( $\tau_{xy}$ )	std( $\tau_{xy}$ )
Conventional $F_C$	4	0.5845	46.0645	6.3739
Proposed $F_C$	4	0.3856	46.6068	4.4636
	$r_c = 3.5$			
	mean( $n$ )	std( $n$ )	mean( $\tau_{xy}$ )	std( $\tau_{xy}$ )
Conventional $F_C$	4	0.6929	85.7490	14.5836
Proposed $F_C$	4	0.3310	86.3288	6.5697
	$r_c = 4$			
	mean( $n$ )	std( $n$ )	mean( $\tau_{xy}$ )	std( $\tau_{xy}$ )
Conventional $F_C$	4	0.5758	146.8792	21.1133
Proposed $F_C$	4	0.3727	147.2594	13.3966



Table 2: Couette flow,  $\eta$  and  $S_c$  as specified inputs,  $\eta = 30$ ,  $S_c = 400$ ,  $m = 1$ ,  $k_B T = 1$ ,  $n = 4$ ,  $\Delta t = 0.01$ , compressibility of water, shear rate of 0.2: Mean and standard deviation of the number density  $n$  and shear stress  $\tau_{xy}$  on the cross section of the flow for several values of  $r_c$  with the proposed ( $\alpha = 1$ ) and conventional conservative forces. For a given  $r_c$ , the variation in the DPD results is significantly reduced with the modified conservative force. Note that different values of  $r_c$  correspond to the same fluid and the “exact” shear stress is 6 (DPD unit). The density fluctuation and the stress error generally increase with  $r_c$  for the conventional  $F_C$ ; in contrast, for the proposed  $F_C$ , the density fluctuation is stable over a wide range of  $r_c$  and errors are much smaller for the shear stress.

$r_c = 2$					
	mean( $n$ )	std( $n$ )	mean( $\tau_{xy}$ )	error( $\tau_{xy}$ ) (%)	std( $\tau_{xy}$ )
Conventional $F_C$	4	0.2140	5.7873	3.5450	0.4293
Proposed $F_C$	4	0.1043	6.0956	1.5933	0.4208
$r_c = 2.5$					
	mean( $n$ )	std( $n$ )	mean( $\tau_{xy}$ )	error( $\tau_{xy}$ ) (%)	std( $\tau_{xy}$ )
Conventional $F_C$	4	0.2672	5.7110	4.8167	0.4688
Proposed $F_C$	4	0.1701	6.1176	1.9600	0.4022
$r_c = 3.0$					
	mean( $n$ )	std( $n$ )	mean( $\tau_{xy}$ )	error( $\tau_{xy}$ ) (%)	std( $\tau_{xy}$ )
Conventional $F_C$	4	0.2964	5.6590	5.6833	0.4119
Proposed $F_C$	4	0.1396	6.0286	0.4767	0.3177
$r_c = 3.5$					
	mean( $n$ )	std( $n$ )	mean( $\tau_{xy}$ )	error( $\tau_{xy}$ ) (%)	std( $\tau_{xy}$ )
Conventional $F_C$	4	0.3958	5.6559	5.7350	0.6375
Proposed $F_C$	4	0.1246	6.0648	1.0800	0.3372
$r_c = 4$					
	mean( $n$ )	std( $n$ )	mean( $\tau_{xy}$ )	error( $\tau_{xy}$ ) (%)	std( $\tau_{xy}$ )
Conventional $F_C$	4	0.3859	5.5519	7.4683	0.4635
Proposed $F_C$	4	0.1464	6.0403	0.6717	0.4576

Table 3: Couette flow,  $\eta$  and  $S_c$  as specified inputs, different viscosity inputs chosen from  $s$  between 0 and 2 (standard value),  $S_c = 400$ ,  $m = 1$ ,  $k_B T = 1$ ,  $n = 4$ ,  $\Delta t = 0.01$ , compressibility of water, shear rate of 0.2: Viscosities predicted by the Kirkwood-Irvin formulation for which both the proposed ( $\alpha = 1$ ) and conventional conservative forces are employed. The former outperforms the latter.

$r_c = 2.5$				
Imposed $\eta$	Conventional $F_C$		Proposed $F_C$	
	Computed $\eta$	Error (%)	Computed $\eta$	Error (%)
47	46.6263	0.79	46.7472	0.53
45	44.4580	1.20	44.8795	0.26
43	42.4131	1.36	42.8948	0.24
41	40.2650	1.79	40.9330	0.16
39	38.3277	1.72	38.8942	0.27
37	36.1052	2.41	36.9136	0.23
35	34.1332	2.47	35.0943	0.26
33	31.9315	3.23	33.1852	0.56
31	29.7771	3.94	31.4797	1.54
$r_c = 3.5$				
Imposed $\eta$	Conventional $F_C$		Proposed $F_C$	
	Computed $\eta$	Error (%)	Computed $\eta$	Error (%)
68	67.7137	0.42	67.8169	0.26
66	65.7913	0.31	65.7371	0.39
64	63.5649	0.67	63.7789	0.34
62	61.5930	0.65	61.9850	0.02
60	59.5492	0.75	59.8873	0.18
58	57.5698	0.74	58.0389	0.06
56	55.5841	0.74	55.8948	0.18
54	53.5671	0.80	53.8571	0.26
52	51.4918	0.97	51.7967	0.39
50	49.3714	1.25	49.8442	0.31
48	47.1981	1.67	47.8911	0.22
46	45.1165	1.92	46.0577	0.12
44	43.0236	2.21	44.0757	0.17
42	41.1593	2.00	42.0830	0.19

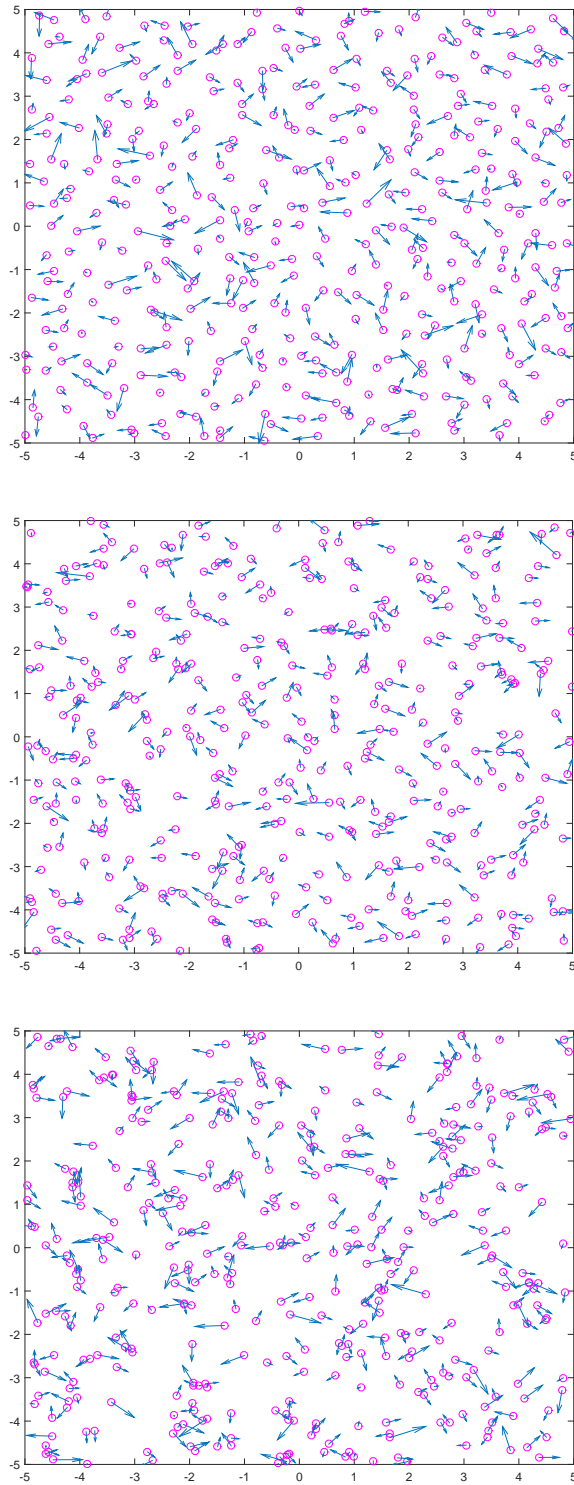


Figure 1: No flow,  $m = 1, k_B T = 1, n = 4, \sigma = 3, \Delta t = 0.01$ , compressibility of water: Instant spatial configurations of DPD particles and their associated velocity vectors for  $r_c = 1 (a_{ij} = 14.30)$  (top) and  $r_c = 2.5 (a_{ij} = 0.91)$  (middle) using the same number of time steps by conventional DPD. The bottom one corresponds to a special case, where  $a_{ij}$  is simply set to 0. Particles tend to form local clusters as  $a_{ij}$  decreases. The arrows denote the particles' velocities.

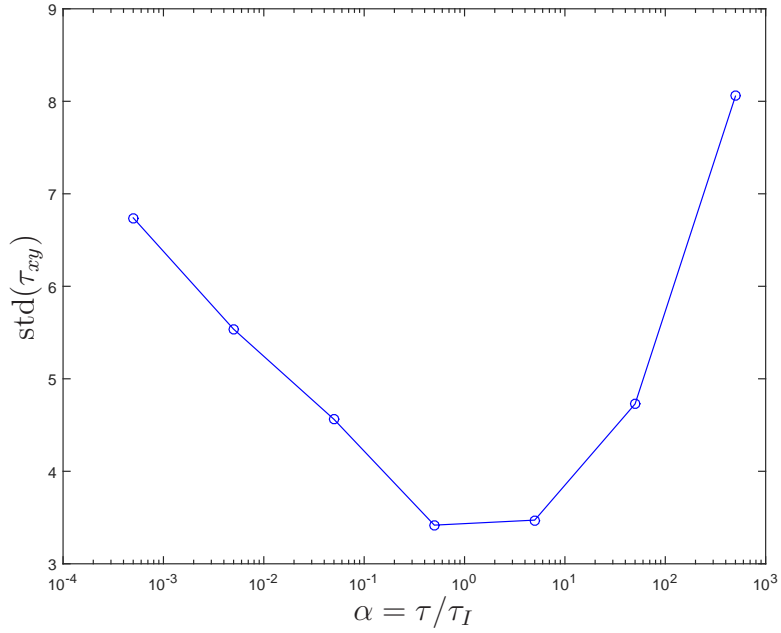
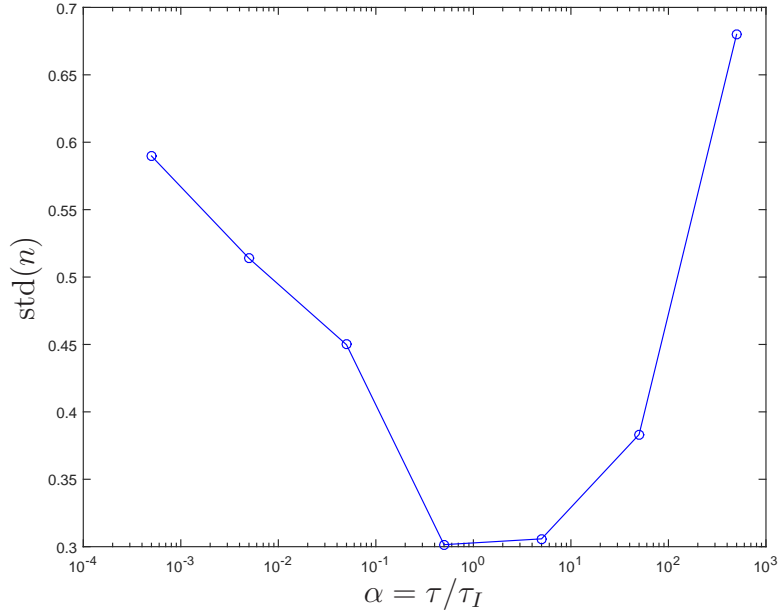


Figure 2: Couette flow, friction coefficient as specified input,  $m = 1, k_B T = 1, n = 4, \Delta t = 0.005, \gamma = 10, r_c = 2.5$ , compressibility of water, shear rate of 0.2: Standard deviations of the number density and shear stress on the cross section against the ratio between two time scales. Too large or too small values of  $\alpha$  result in larger fluctuations in  $n$  and  $\tau_{xy}$ . The best  $\alpha$  is in the range of  $10^{-1}$  to  $10^{+1}$ .

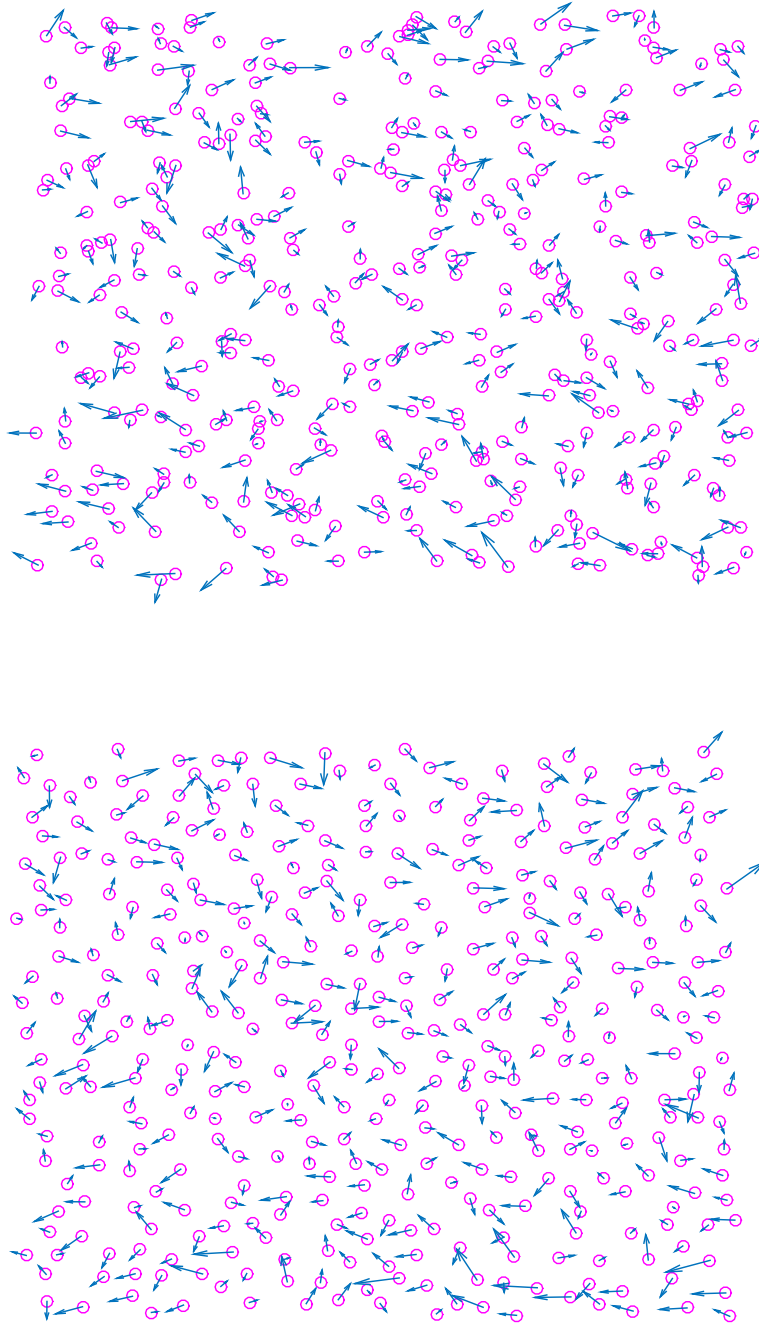


Figure 3: Couette flow, friction coefficient as specified input,  $m = 1, k_B T = 1, n = 4, \Delta t = 0.005, \gamma = 10, r_c = 2.5$ , compressibility of water, shear rate of 0.2: An instant spatial configuration for  $\alpha = 0.0005$  (top) and  $\alpha = 0.5$  (bottom). Particles tend to form local clusters at  $\alpha = 0.0005$ . The arrows denote the particles' velocities.

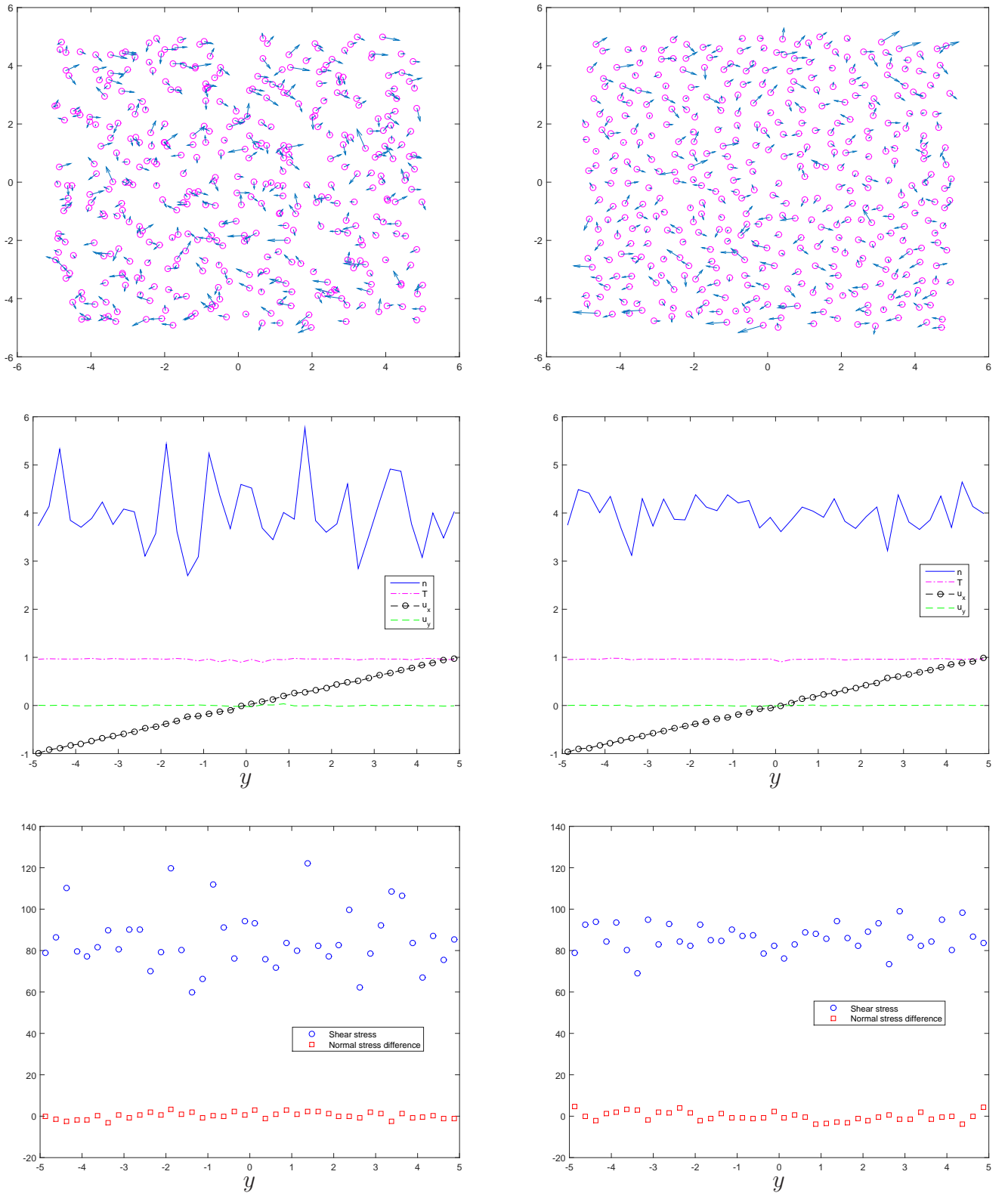


Figure 4: Couette flow, friction coefficient as specified input,  $m = 1, k_B T = 1, n = 4, \Delta t = 0.01, \gamma = 4.5, r_c = 3.5$ , compressibility of water, shear rate of 0.2: DPD results with the convention (left,  $\alpha = 212$ ) and proposed (right,  $\alpha = 1$ ) conservative forces. A clear improvement is achieved for spatial configuration (top), number density (middle) and shear stress (bottom).

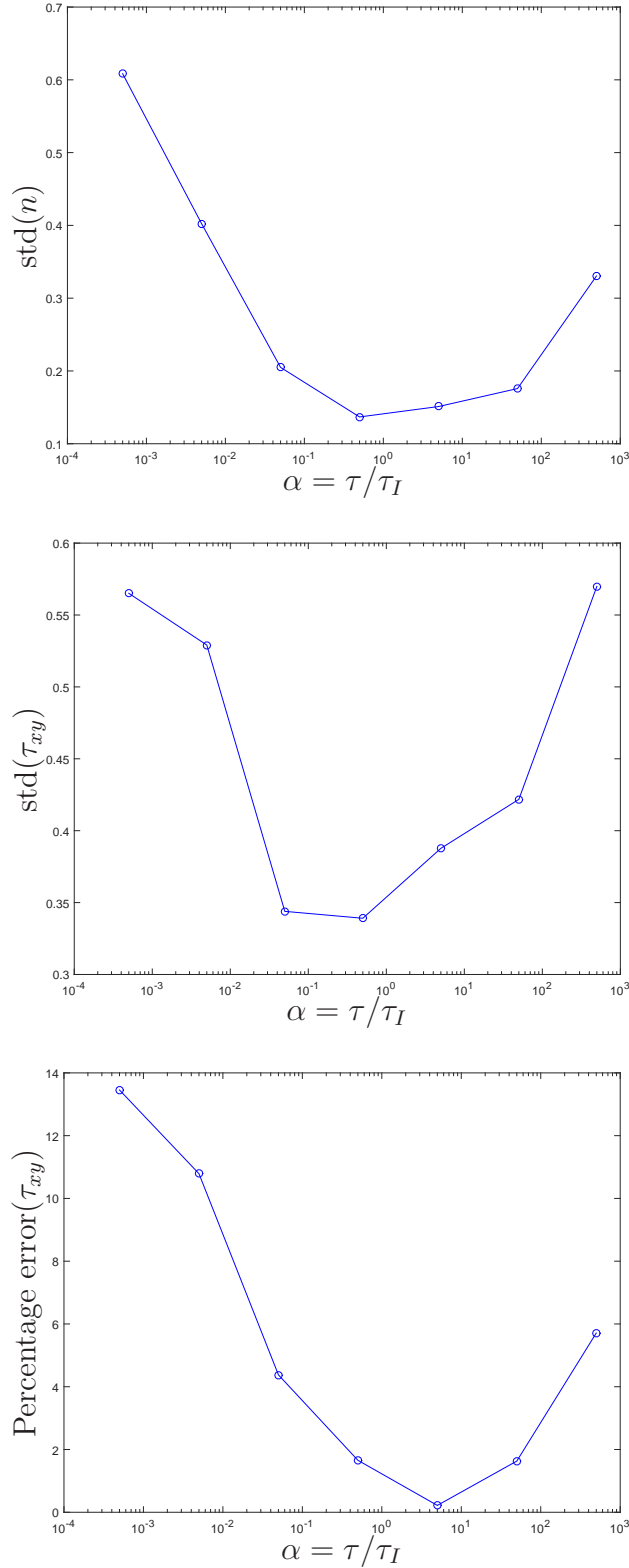


Figure 5: Couette flow,  $\eta$  and  $S_c$  as specified inputs,  $\eta = 30, S_c = 400, r_c = 2.5, m = 1, k_B T = 1, n = 4$ , compressibility of water, shear rate of 0.2: Standard deviation of the number density  $n$  and shear stress  $\tau_{xy}$  on the cross section of the flow for several values of  $\alpha = \tau/\tau_I$ . It is noted that the “exact” shear stress is 6 (DPD unit) and percentage errors of  $\tau_{xy}$  against  $\alpha$  are also displayed. For  $\alpha$  from  $5 \times 10^{-3}$  to  $5 \times 10^2$ ,  $\Delta t$  is chosen as 0.01. For  $\alpha = 5 \times 10^{-4}$ , to maintain the satisfaction of the Boltzmann temperature,  $\Delta t$  is reduced to 0.005. Minimum values of the variations and percentage errors occur within the range of  $10^{-1}$  and  $10^1$ .

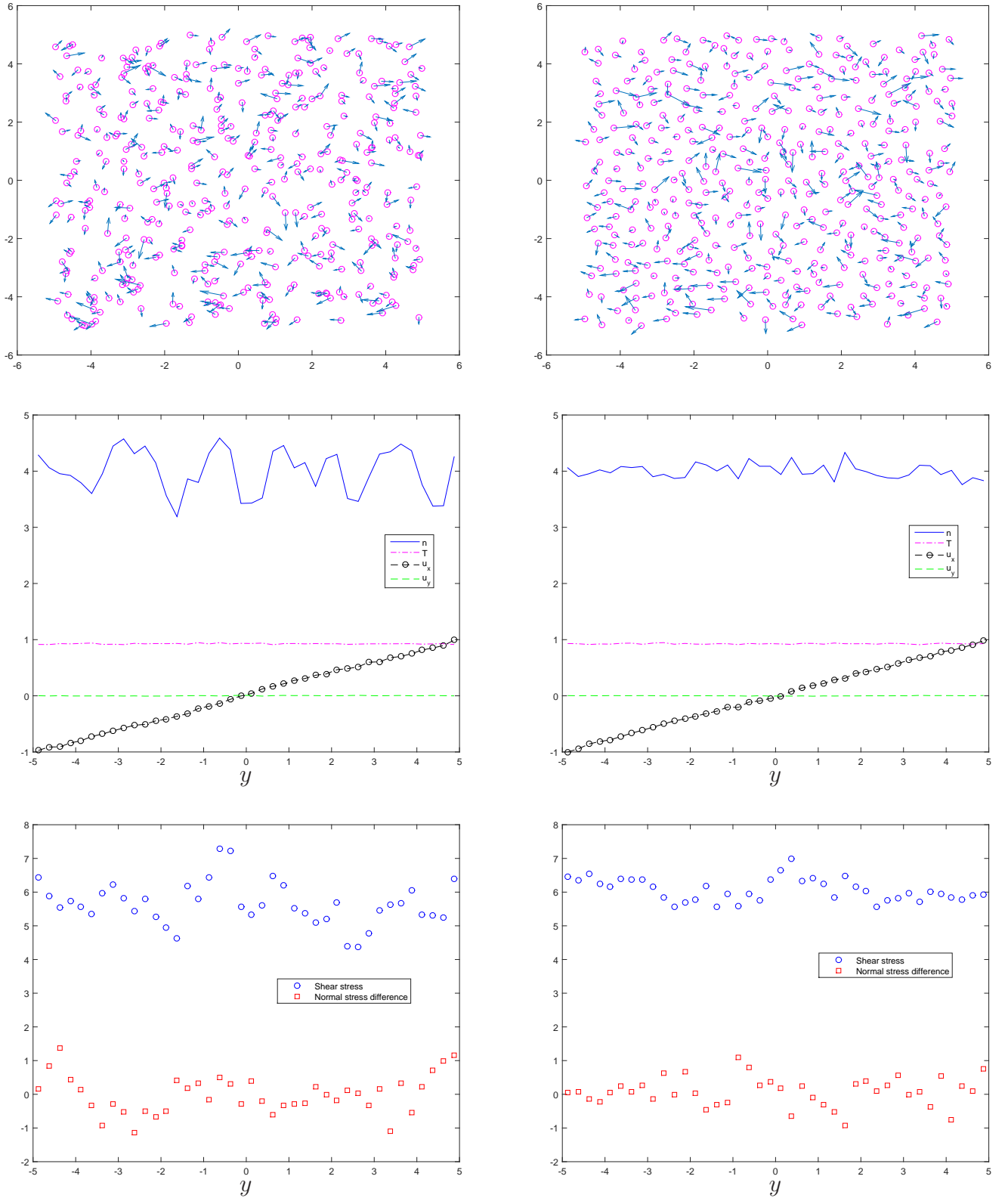


Figure 6: Couette flow,  $\eta$  and  $S_c$  as specified inputs,  $\eta = 30, S_c = 400, r_c = 3.5, m = 1, k_B T = 1, n = 4, \Delta t = 0.01$ , compressibility of water, shear rate of 0.2: DPD results using the same number of time steps with the convention (left,  $\alpha = 1717$ ) and proposed (right,  $\alpha = 1$ ) conservative forces. A clear improvement is achieved for spatial configuration (top), number density (middle) and shear stress (bottom). In comparison with Figure 4, for the same  $r_c$ , DPD results with  $\eta$  and  $S_c$  as specified inputs are superior (i.e. smaller density fluctuations) to those with  $\gamma$  as a specified input.